Title
Determination of motility forces on isolated chromosomes with laser tweezers

Permalink
https://escholarship.org/uc/item/5w0248s2

Journal
Scientific Reports, 4(1)

ISSN
2045-2322

Authors
Khatibzadeh, Nima
Stilgoe, Alexander B
Bui, Ann AM
et al.

Publication Date
2014

DOI
10.1038/srep06866

Peer reviewed

Determination of motility forces on isolated chromosomes with laser tweezers

Nima Khatibzadeh[1], Alexander B. Stilgoe[2], Ann A. M. Bui[2], Yesenia Rocha[1], Gladys M. Cruz[1], Vince Loke[2], Linda Z. Shi[3], Timo A. Nieminen[2], Halina Rubinsztein-Dunlop[2] & Michael W. Berns[1,3]

[1]Beckman Laser Institute and Medical Clinic, University of California, Irvine, 1002 Health Sciences Road, Irvine, CA 92612, USA, [2]School of Mathematics and Physics, The University of Queensland, St. Lucia, QLD, 4072, Australia, [3]Institute of Engineering in Medicine, University of California, San Diego, 9500 Gilman Drive, La Jolla, California 92093, USA.

Quantitative determination of the motility forces of chromosomes during cell division is fundamental to understanding a process that is universal among eukaryotic organisms. Using an optical tweezers system, isolated mammalian chromosomes were held in a 1064 nm laser trap. The minimum force required to move a single chromosome was determined to be ≈0.8–5 pN. The maximum transverse trapping efficiency of the isolated chromosomes was calculated as ≈0.01–0.02. These results confirm theoretical force calculations of ≈0.1–12 pN to move a chromosome on the mitotic or meiotic spindle. The verification of these results was carried out by calibration of the optical tweezers when trapping microspheres with a diameter of 4.5–15 μm in media with 1–7 cP viscosity. The results of the chromosome and microsphere trapping experiments agree with optical models developed to simulate trapping of cylindrical and spherical specimens.

T he first study to measure the force exerted on a chromosome during cell division was performed on grasshopper spermatocytes[1]. In that study a microneedle was used to impale the chromosome through a stretched cell membrane. The force at which the chromosome stopped moving was determined to be 700 pN[1]. However, theoretical calculations by several investigators have placed the force values for moving chromosomes at 0.1–12 pN[2–5]. More recently, the non-invasive method of optical tweezers (optical trapping) was used for direct measurement of forces on chromosomes[6].

Optical trapping is a precise technique to manipulate objects with length scales from tens of nanometers to hundreds of micrometers, and measure forces from few to several hundreds of piconewtons[7]. Given that it is non-invasive and non-destructive[8], optical traps have been used in a multitude of biological studies, such as, the determination of motility forces of kinesin[9,10], human spermatozoa swimming force[11], forces associated with cell adhesion[12] and organelle transport[13], compliance of bacteria flagella[14], and mechanical[15] and electromechanical properties of cellular plasma membranes[16].

In optical tweezers studies of forces exerted on a chromosome during cell division[6] the resulting forces of 3–35 pN approached, but did not match, the predicted theoretical calculations and were orders of magnitude less than 700 pN. The significance of the optical trapping experiments is that there was no physical contact between the force measurement probe and the chromosomes, hence stretching of the plasma membrane to reach the chromosomes, as was necessary in the early invasive microneedle study[1], was avoided[6]. In this study[6], chromosome movements were stopped by the optical trap. The power needed to prevent the chromosome from escaping the trap was determined. The usual method of calibrating an optical trap to determine the lateral escape force is to use movement of the stage to produce fluid flow past the trap, exerting an increasing viscous drag force on the trapped particle until the particle escapes the trap[17,18]. However, this requires the trapped particle to be able to freely move relative to its surroundings, which is not possible for a chromosome within a cell. In addition, it also requires knowledge of the viscosity of the surrounding medium. As this cannot be easily performed within the cell, the corresponding forces were estimated by assumption of a range of values for chromosomes trapping efficiency that was based on previous chromosome fragment trapping experiments[8], and experiments to trap sperm heads after removal of their tails[11,19].

Since the optical trapping values were still somewhat higher than the predicted theoretical ones, we conducted a study to more precisely determine the escape force for a trapped isolated chromosome, outside the cell. In

addition, it has been suggested that the differences in force measurements on chromosomes between the early needle-invasive study[1] and the recent non-invasive optical tweezers studies[6] was due to some unknown photo-damage effects of the laser[20]. There does not appear to be any good basis for that claim, considering the wide range of biological studies conducted with optical tweezers at irradiances considerably higher than the ones reported in the recent chromosome trapping studies[6]. At the wavelength (1064 nm) and power used (too low for non-linear effects), no significant photochemistry is to be expected, and the only important effect would be due to heating generated by absorption of the 1064 nm light by water. Since we can expect heating by about 1 K/100 mW[21–25], no significant heating is expected. However, it is straightforward to investigate the effect of heating during the measurement of the escape force, since the viscosity of water, and hence the drag force, varies with temperature.

In the present study we have performed systematic experiments and theoretical simulations to determine the optical trapping forces on isolated single chromosomes, and analyzed the force-power relationship in order to determine the trapping efficiency factor, Q. This calibration procedure to find the escape force (or escape Q) was performed using the same optical tweezers system as used for the measurements on chromosomes within the cell. Therefore, most features of the trap are identical between the experiments inside and outside the cell: aberrations, focusing of the beam, etc. For experiments inside the cell, the only difference in the trap will be due to propagation of the beam through the cell. Since the refractive index of the cell is close to that of its surroundings, the effect will be minor; the most likely effect would be to produce a larger focal spot, reducing the escape force. That the effect on the focal spot will be small is evident due to the fact that we can clearly view the interior of the cell with the microscope. In addition, if the refractive index inside the cell is higher than that of the medium surrounding the isolated chromosome, the escape force would also be reduced. Therefore, measurements on isolated chromosomes can be assumed to give an upper limit to the escape force within the cell.

First, it is important to test the calibration procedure. In order to do this, the escape force measurement was performed on polystyrene microspheres 4.5–15 microns in diameter. A range of powers and viscosities of the surrounding medium were used. A range of powers allows observation of the effects of heating; if there is significant heating, the viscous drag for a given flow speed will decrease, and a higher flow speed is required for the object to escape the trap (at about 35°C, a temperature change of 5°C will change the viscosity by about 10%). In addition, the escape path of a trapped particle affects the escape force[26], and this can be affected by the rate at which the ratio of viscous drag to optical force increases. Varying the power and viscosity allow this ratio to be varied, checking for effects on the calibration of the trap. These measurements provided a verification of the calibration of the system and its independence from variation in power and viscosity of the medium.

Since size, shape, and refractive index of the microspheres were known, the optical forces acting on them could be predicted theoretically. The microsphere trapping experiments were simulated by an optical model calculating forces and trapping efficiency of microspheres using the T-matrix method. This allowed the development of an accurate model of the trap, including the effects of aberrations.

Next, chromosomes from Chinese hamster ovary (CHO) cells were isolated using standard procedures[27] and optically trapped with a range of *in situ* trapping powers. Trapping forces on isolated chromosomes were calculated based on Stokes' equation for cylinders, followed by determination of chromosome trapping efficiency at each trapping power. Measurements were made for two different viscosities.

Using electromagnetic field calculations for cylindrical objects, an optical model was constructed to simulate trapping of isolated chromosomes at 1064 nm, and to determine the optical forces and trap-

ping efficiency of the chromosomes. Our experimental results and numerical simulations on isolated chromosomes confirm that the amount of force necessary to move a single chromosome on the spindle is in the range of 0.1–12 pN.

Results

Trapping of microspheres. Polystyrene microspheres with diameters of ≈4.5–15 μm were trapped at 1064 nm in a range of *in situ* powers and in media with varying viscosity of 1–7 cP. At each trapping power, trapping forces exerted on the microspheres were determined using the viscous drag method described in the Microsphere trapping of the Methods section. Briefly, the particle (microsphere or chromosome) escapes the trap when the viscous drag force is greater than the optical trapping force. Based on the Stokes' equation, the viscous drag force exerted on a sphere in a fluid flow with very low Reynolds numbers (Re≪1) can be calculated by the following equation:

$$F_{drag} = 6\pi\mu r v \beta \tag{1}$$

F_{drag} is the viscous drag force (N), μ is the dynamic viscosity (N.s/m²) of the surrounding media, r is the radius of the microsphere (m), v is the velocity of the fluid flow (m/s) at which the microsphere escapes the trap in our experiments. β is a correction factor for the viscous drag force arising from proximity of the trapped microsphere to the surface of the petri dish and can be calculated from the following equation[17]:

$$\beta = \lfloor 1 - \frac{9}{16}(r/h) + \frac{1}{8}(r/h)^3 - \frac{45}{256}(r/h)^4 - \frac{1}{16}(r/h)^5 \rfloor^{-1} \tag{2}$$

where h (≈20 μm in our experiments) is the distance from the glass surface to the center of the trapped microspheres.

The calculated trapping forces versus trapping powers are shown in Fig. 1a for 4.5 μm microspheres suspended in 3 and 7 cP surrounding media. As seen in this figure, the trapping forces increased as the trapping power increased. This was the case for all viscosities. The force values were a linear fit to power ($R^2 = 0.99$). This indicates that no unusual heating occurred.

The trapping force is correlated with the trapping power by the following equation[17,28]:

$$F = \frac{QPn}{c} \tag{3}$$

F is the total trapping force (N), P is the incident laser power at the specimen (W), c is the speed of light (m/s) in a vacuum, and n is the refractive index of the surrounding medium. The parameter $|Q|$ is the dimensionless trapping efficiency which indicates the fraction of the incident light momentum transferred to the trapped object and varies from 0 to 2[18,28]. Using Eq. 3 and the escape velocities, the maximum transverse trapping efficiency (Q_{Escape}) of the trapped microspheres were calculated at each trapping power. The values of Q_{Escape} versus trapping power in the range of ≈20–60 mW are shown in Fig. 1b. Based on these measurements, Q_{Escape} is independent of trapping power and media viscosity in the ranges examined.

For calibration purposes, trapping experiments were repeated on microspheres with diameters of 10 and 15 μm over a range of trapping powers, and in media with viscosities of 1–7 cP. The trapping forces increased linearly with trapping powers similar to that seen with the 4.5 μm diameter microspheres. The values of Q_{Escape} remained unchanged at different trapping powers and were independent of the media viscosity, but increased with the diameter of the trapped microspheres. Values of Q_{Escape} obtained from trapping experiments for microspheres with different sizes are summarized in Table 1.

Simulation model of trapped microspheres. The verification of the escape forces exerted on microspheres was investigated by a
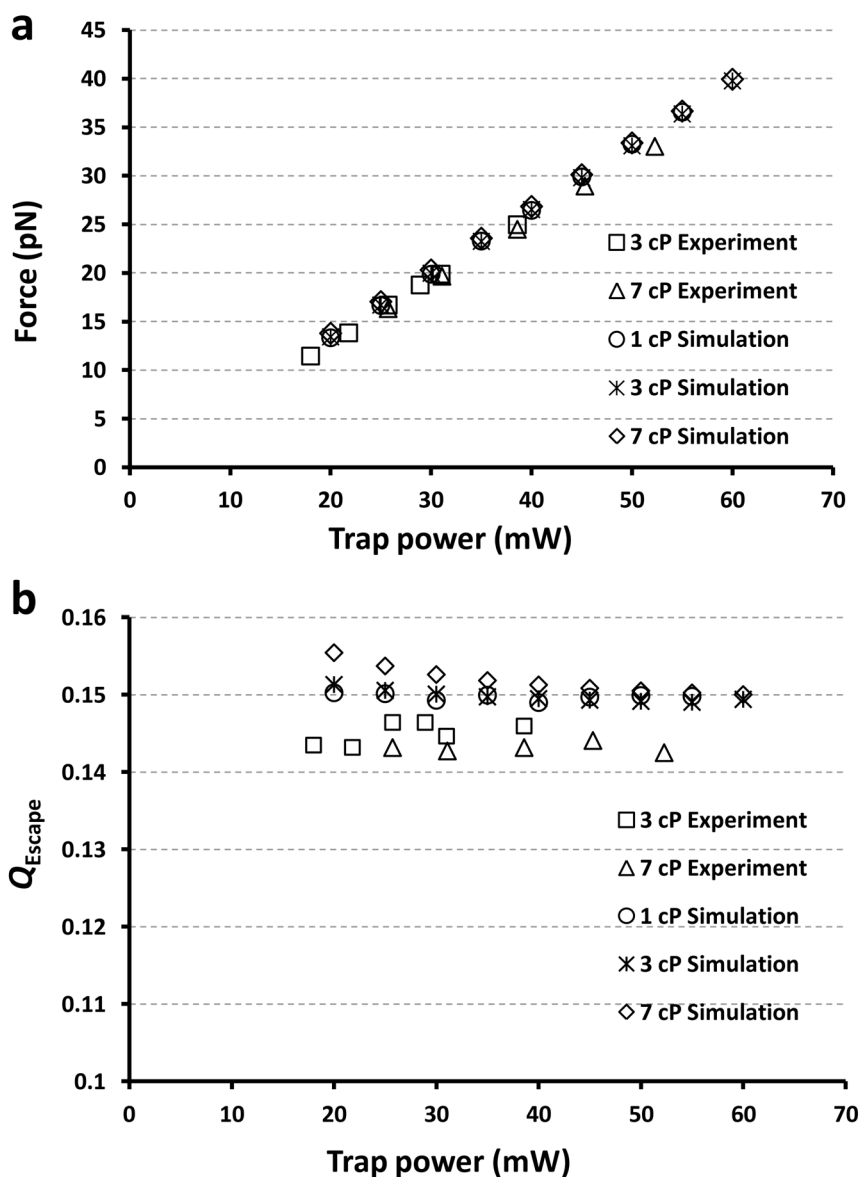
Figure 1 | Experimental and numerical simulation results for optical trapping of microspheres. (a), Trapping force-power measurements for 4.5 μm polystyrene microspheres trapped at 1064 nm wavelength. (b), Maximum transverse trapping efficiency (Q_{Escape}) versus trapping power for 4.5 μm polystyrene microspheres trapped at 1064 nm wavelength.

numerical simulation model. The simulation used the optical tweezers toolbox with the T-matrix method to calculate the optical forces on microsphere in the trap[29,30]. This model described by equation 4 recreated the experiment. The microsphere is initially at the equilibrium position of the trap. The microscope stage is moved in a transverse direction with a linearly increasing velocity, which moves the microsphere out of the trap. The time interval, Δt in equation 4 is defined such that x_i - x_{i-1} is not too large, less than

0.5% of the particle radius, so that the optical force does not change too greatly. In order to reproduce the experimental results of the escape trajectories of the microspheres it is important to consider not only the optical forces but also viscous and mechanical forces. The behavior of the particle in a fixed orientation is modeled using the following equation:

$$x_i = x_{i-1} + \left(\Gamma^{-1}[f_o(x_{i-1}) + g] + v_{i-1}\right)\Delta t \qquad (4)$$

Table 1 | Calculated values of maximum transverse trapping efficiency (Q_{Escape}) (mean ± s.d.) for microspheres with different diameter sizes suspended in surrounding media with various viscosity values

	Microsphere diameters (μm)		
Surrounding media viscosity (cP)	4.5	10	15
1	Not determined	0.1934 ± 2.4e-3	0.23 ± 3e-3
3	0.1436 ± 0.003	0.1923 ± 2e-3	0.2313 ± 1.5e-3
7	0.1431 ± 6e-4	0.1898 ± 2.2e-3	0.2291 ± 2.8e-3

where the particle is moved from its current position to a new position by the sum of the forces acting on it. The forces in our simulation model are: the optical force created by the optical tweezers, $f_o(x_{i-1})$; the buoyancy force of the particle, g; and viscous drag force due to fluid flow around the particle. The drag force is generated in response to movement of the stage at velocity v_{i-1} giving rise to a force value of Γv_{i-1} where Γ is the drag tensor. Eq. 4 is obtained assuming motion at terminal velocity such that the total force is equal to $\Gamma(x_i - x_{i-1})\Delta t$. As the sphere is displaced in the optical trap by the flow, it also experiences an optically induced torque which changes the orientation as a function of time. The simulation also accounts for rotational drag; this doesn't affect the motion of the spheres, due to their rotational symmetry, but is important for chromosomes. Brownian motion of the trapped particle is ignored in this simulation model. The particle should escape the trap when the external forces overcome the optical force. The escape force is taken to be the greatest radial optical force acting on the particle during the escape process wherein the particle moves from the centre toward the outside of the optical trap. The values of the escape forces obtained from the simulation model are shown in Fig. 1a versus trapping power for 4.5 μm diameter microspheres suspended in media with 1–7 cP viscosity. The corresponding values of Q_{Escape} obtained from the simulation model for 4.5 μm diameter microspheres are shown in Fig. 1b.

Trapping of chromosomes. Individual whole metaphase chromosomes isolated from Chinese hamster ovary (CHO) cells were optically trapped with a 1064 nm laser tweezers. Metaphase chromosomes are elongated cylinders of condensed chromatin with relatively smooth surfaces. Recent reports have determined the length-to-diameter ratio of chromatids vary between ≈9–19 with an average value of ≈13[31]. Consistent with these observations, the average length-to-radius ratio of the metaphase CHO chromosomes in our experiments is ≈14 (see the Phase contrast imaging and chromosome size measurements in the Methods section).

Using the viscous drag method, escape velocities of the individual trapped chromosomes were measured at each trapping power as described in the Chromosome trapping of the Methods section. Optical forces exerted on chromosomes by laser tweezers were calculated based on hydrodynamics of long slender bodies according to Stokes flow equations (Eqs. 5–6):

$$F_\perp = \frac{4\pi\mu v L}{\ln\frac{L}{a} + 0.193 - \frac{3L}{8h}} \tag{5}$$

$$F_\parallel = \frac{2\pi\mu v L}{\ln\frac{L}{a} - 0.807 - \frac{3L}{16h}} \tag{6}$$

where $F_\perp$ and $F_\parallel$ are the forces on the cylinder with the fluid flow normal and parallel to the cylinder longitudinal axis, respectively. The parameter μ is the dynamic viscosity of the surrounding media (N.s/m²), v is the fluid flow velocity (m/s) at which the chromosome escapes the trap, parameters L and a are the length and radius of the cylinder (m), respectively, and h is the distance of the center of the chromosome from the bottom surface[32]. These equations have been used in motion studies of other biological slender bodies at low Reynolds numbers, e.g. in eukaryotic ciliary motion[32], propulsion in Escherichia and Salmonella flagellated bacteria[33], mechanics of discharge of ascospores in Giberella zeae[34,35], and growth of cellular protrusions[36].

The corresponding trapping force-power measurements of individual chromosomes for a range of the trapping powers and in media with 1–3 cP viscosity are shown in Fig. 2a. The trapping forces on the chromosomes linearly increased with the trapping powers at each

individual viscosity as shown by linear regressions represented by the dashed red lines on Fig. 2a.

Using the trapping force-power measurements of the individual chromosomes, the transverse trapping efficiency of the chromosomes was calculated at each trapping power based on Eq. 3. Since the force measurements were performed at the escape velocity at which the chromosomes left the trap, the Q in our measurements is equivalent to the maximum transverse trapping efficiency and is denoted as Q_{Escape}. The Q_{Escape} values of the chromosomes versus the trapping power for experiments performed in 1 and 3 cP media are shown in Fig. 2b. At each media viscosity the Q_{Escape} is independent of the trapping power as there are no statistically significant changes between the Q_{Escape} values at different trapping powers. Thus, it is safe to assume that no unusual heating occurred. The Q_{Escape} values are higher for chromosomes trapped in 3 cP media compared with the ones trapped in the 1 cP media. The mean ± s.d. value of the Q_{Escape} for the trapped chromosomes in 1 and 3 cP media are respectively, ≈0.011 ± 0.002, and ≈0.019 ± 0.005. This variation indicates that escape trajectory differed for the different viscosities.

Simulation model of trapped chromosomes. Chromosomes at metaphase have a cylindrical structure[31,37,38] of densely packed chromatin. The optical properties of homogenous cylindrical structures can be modeled using calculations of electromagnetic field theory and the behavior of such objects influenced by optical tweezers can be determined. Using an optical tweezers calculation package[29,30] we constructed an optical model of chromosomes using nano-cylinders with refractive indices of 1.36 and 1.4, radius of 500 nm, and length of 6 μm. Using this model, we calculated optical forces acting on a trapped cylinder when dragged from the center of an optical trap. Alignment torques arising from the optical tweezers will tend to change the orientation of the cylinder. Fig. 3 shows the results of the optical chromosome model using two trajectories. Fig. 3a where the trapped chromosome is dragged perpendicular to the trapping laser and in Fig. 3b the chromosome is dragged along the optical axis of the laser beam. This configuration constitutes the 'best' and 'worst' cases of chromosome trapping. Due to the viscosity dependence observed in the chromosome escape experiments, it is important to consider the limiting cases. The actual escape trajectory is likely somewhere between these two extreme trajectories and at a slight angle to the lengthwise escape trajectory. Since the simulation includes both optical and drag forces and torques, the orientation of the chromosome varied during the simulated escape. The peak transverse restoring force of the optical tweezers, the escape force, corresponds to the escape Q of $|Q_{Escape}| \approx 0:019$–0.028 as calculated in the model (Fig. 3c) for the chromosomes leaving the trap in horizontal orientation. For vertical escape, the Q_{Escape} varies between 0.013 and 0.019 (see Fig. 3d). These theoretical results agree well with the experimental findings of $|Q_{Escape}| \approx 0:019$. This value lies between the 'best' and 'worst' case orientations discussed above; this supports our expectation that the real escape is between these limiting cases. A result of this dynamic simulation (including Brownian motion) is shown in Fig. 4. In this simulation we use the same parameters as in figure 3. The escape Q (Q_{Escape}) in x direction is ≈0.023, which compares well with experimental results. An animation simulating the escape of a trapped chromosome from the optical tweezers is provided as Supplementary Movie M1.

Discussion

Optical trapping and determination of forces on the isolated chromosomes. The motion of chromosomes during cell division (mitosis or meiosis) is mediated by the forces exerted on their kinetochores via microtubules and associated proteins, and quantitative measurement of these forces is fundamental to understanding a biological phenomenon that is universal among
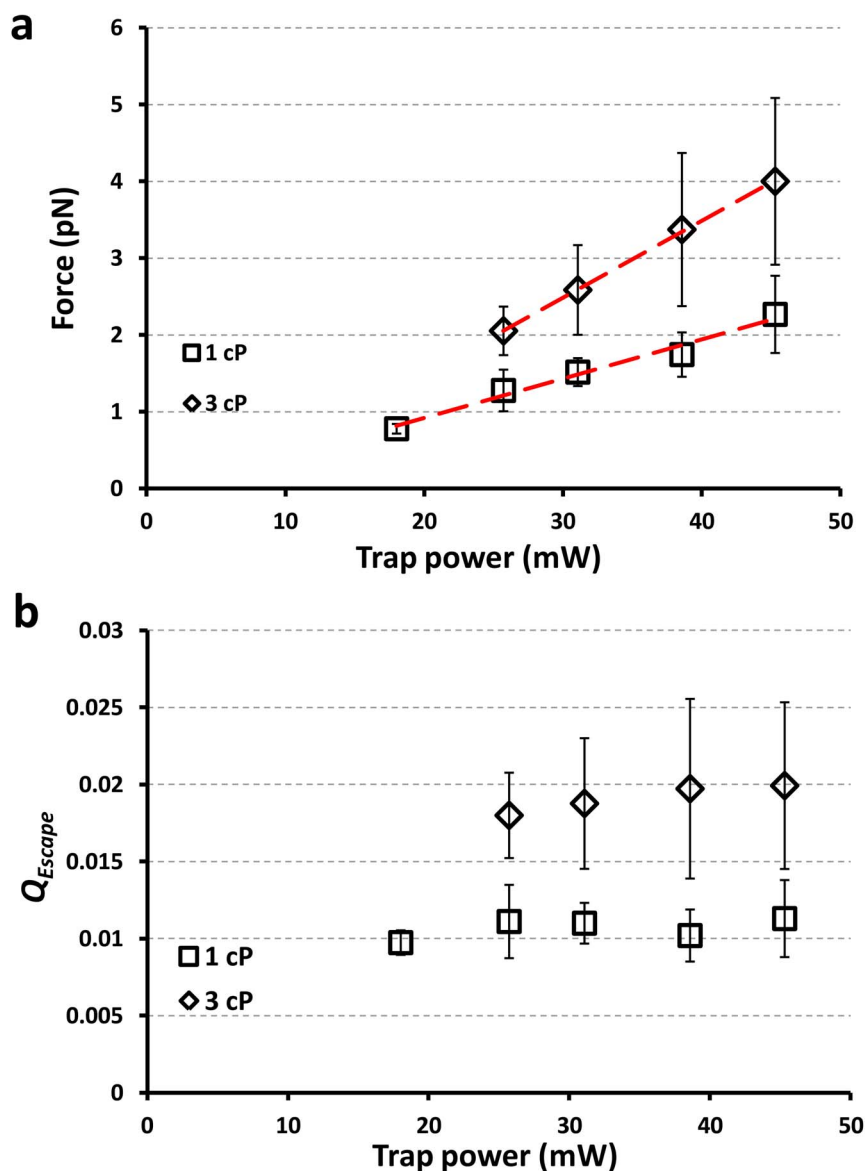
Figure 2 | Optical trapping of isolated chromosomes. (a), The trapping force-power measurements of the isolated individual CHO chromosomes suspended in 1 and 3 cP viscous media and trapped at 1064 nm wavelength. (b), Calculated maximum transverse trapping efficiency (Q_{Escape}) versus trapping power for individual CHO chromosomes suspended in 1 and 3cP viscous media and trapped with 1064 nm wavelength laser tweezers.

eukaryotic organisms. This leads to the importance of employing both an experimental technique, and a simulation model, to determine the forces exerted on chromosomes.

Given its extensive biological application, optical tweezers is an ideal technique to study the dynamics of chromosomes inside a live cell during cell division and, particularly, to quantitate the associated motility forces. These forces can be calculated by measuring the *in situ* trapping powers required to stop the chromosomes, as long as the trapping efficiency (Q) of the chromosomes is known. Therefore, knowledge of Q is essential. Since the number of kinetochore microtubules can change throughout the cell division process[39,40], and the velocity of chromosomes can be ten times faster in prometaphase compared to anaphase[20], it is likely that different amounts of forces are exerted on the chromosomes at different phases of the mitotic/meiotic process. Therefore, trapping of chromosomes in order to quantify these forces will require different *in situ* trapping powers at different stages of cell division. For this reason, we studied trapping behavior of isolated chromosomes in a wide range of *in situ* powers used in other biological studies such as trapping single kinesin molecules (15–63 mW)[41], buckling and trapping of microtubules (1–25 mW)[42], and trapping kinetochores in mesostoma (5–23 mW) and crane-fly spermatocytes (28–65 mW)[6].

Assuming similar trapping properties for the objects under study, knowledge of the trapping efficiency of objects at a given wavelength enables calculation of the optical trapping forces at a given trapping power. In a recent study measuring motility forces on chromosomes inside live cells using optical tweezers[6], the value of Q for chromosomes was assumed to be between ≈0.06–0.16. This resulted in calculated force values of 3–12 pN for prometaphase mesostoma spermatocyte chromosomes and 6–35 pN for prometaphase and anaphase crane-fly spermatocytes. A Q value of 0.06 was calculated based on a previous report where 440 mW laser power was needed to trap chromosome fragments with an associated trapping force of 30 pN[8]. However, the power measurement reported in that study was likely before the objective lens rather than at the laser focal point inside the cell. Additionally, in a study trapping tail-less primate sperm heads, which are morphologically different than chromosomes, a Q of 0.16 was reported[11].

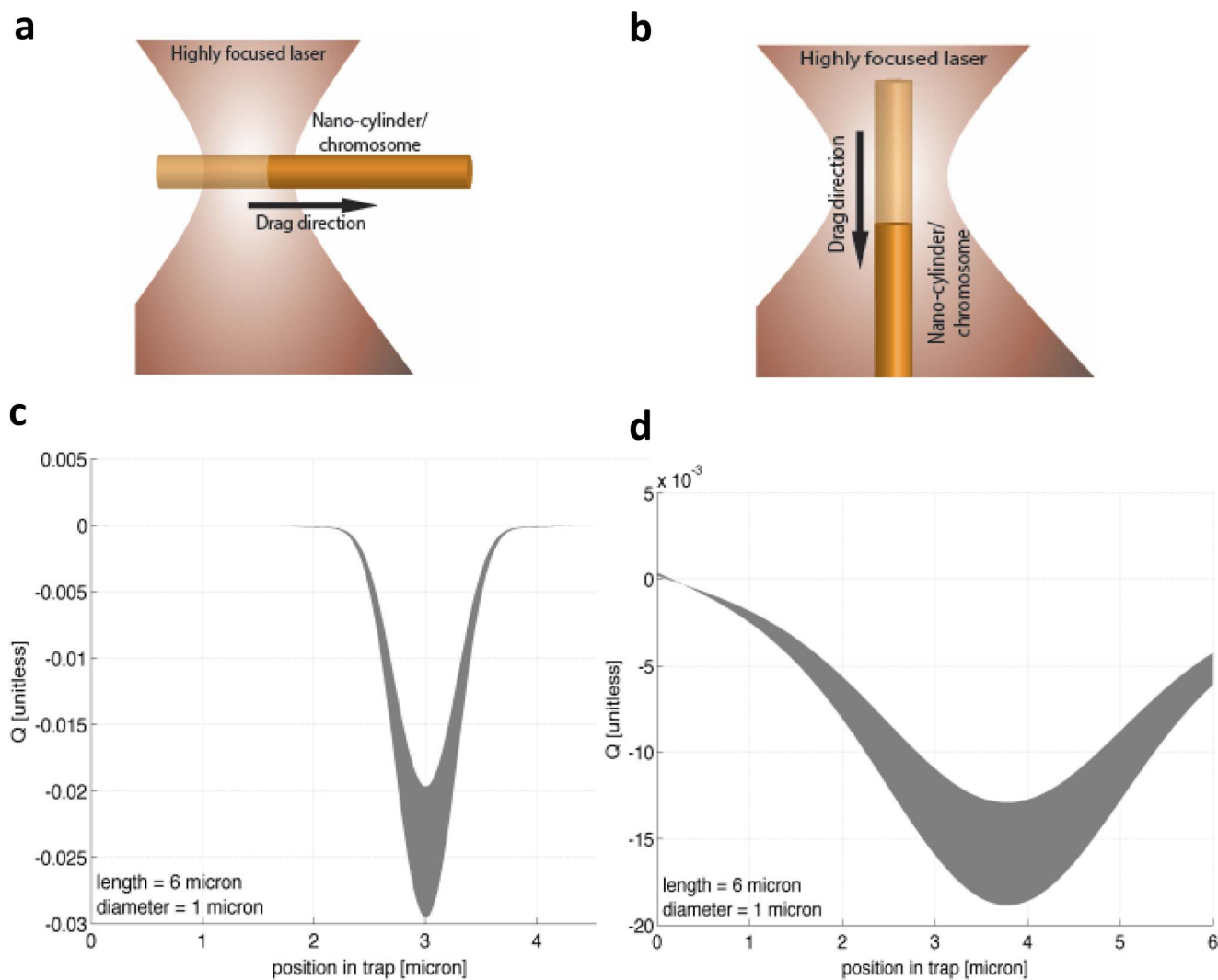**a**

b

c

d

Figure 3 | Optical model of chromosomes using glass nano-cylinders. (a) and (b) show schematics of escape trajectories of optically trapped cylinders with their long axes aligned with the drag directions. (c) and (d) show the Q_{Escape} of glass nano-cylinders corresponding to the schematics shown in a and b, respectively, as a function of displacement from the trapping center. The shaded region of the force curves illustrates the variation in the trap strength with refractive index between 1.35 and 1.36. The glass nano-cylinders have radius of 500 nm, and length of 6.0 μm.

In our study, the Q_{Escape} values for chromosomes are directly measured based on their trapping force-power measurements at 1064 nm. They also are calculated using a simulation model. Our simulations were done taking into account the considerations of optical aberrations in the microscope and the depth of the trap. Using both experimental and theoretical approaches, the values are in the range of ≈0.01–0.02 which is somewhat lower than ≈0.06–0.16 previously suggested[6]. Our results, however, are consistent with smaller force values for chromosome movements. They are closer to the theoretical values of 0.1–0.7 pN[3–5] and 12 pN[2] reported as necessary to move anaphase and prometaphase chromosomes, respectively. These values are considerably smaller than the 700 pN force that caused chromosome velocity to fall to zero inside anaphase grasshopper spermatocyte using a microneedle to impale the chromosome through the stretched cell membrane[1]. As recently discussed, it is conceivable that in the microneedle experiments, a high force measurement artifact arose from stretching the cell membrane to hook the chromosomes. In the experiments where atomic force microscopy was used for force measurements the force values obtained were of the order of ≈200–900 pN in response to indenting the membrane by 0.5–1 μm[43–45]. Thus, forces of this magnitude would be expected in

the earlier experiments on chromosomes where the microneedle caused indentation of the cell membrane.

Our trapping experiments are performed with media viscosity values between 1–7 cP which is within the range of the 1–3 cP reported for microviscosity of the aqueous phase of the cytoplasm in mammalian cells[46–50]. These values have been reported to increase to as high as 140 cP in cellular vesicles[51]. The average viscosity value reported for the cell cytoplasm surrounding the mitotic spindle is ≈300 cP[2,5,52], and in a more recent study it was reported as high as ≈1200 cP[53]. The average velocity of chromosome movement during anaphase is ≈1 μm/min[20] but can be five times higher in some cells. Given the maximum average velocity of 5 μm/min, and published viscosity values as high as 1200 cP, the corresponding viscous drag forces exerted on the chromosomes estimated by Eqs. 5 and 6 would only be up to ≈3 pN. This lies within the range of the forces measured in this study.

Trapping efficiency of the isolated chromosomes and microspheres. The validity and quantitative accuracy of the drag force calibration method used here has been confirmed by testing the method with microspheres. The computational model used to simulate the escape from the trap has been demonstrated to give optical forces in close
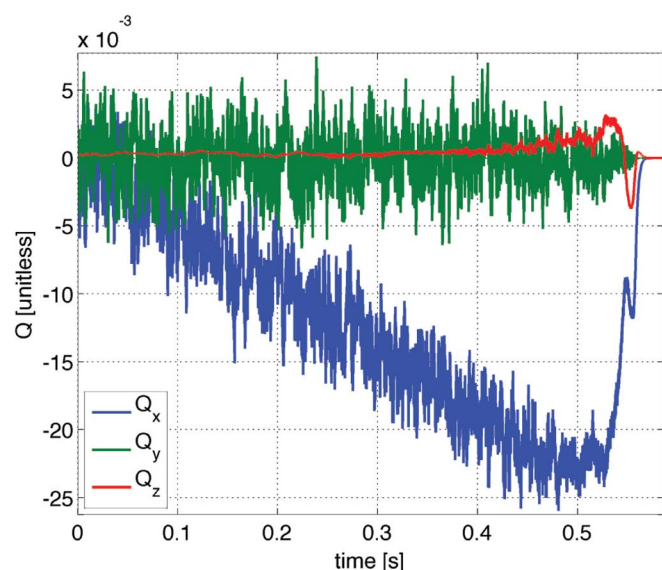
Figure 4 | Numerical simulation of the opto-visco-mechanical chromosome model. The numerical simulation reproduces the escape trajectory in the presence of Brownian motion using parameters directly obtained from the experiment. The initial equilibrium orientation is found and the cylinder (refractive index of 1.36, diameter of 1 μm, and length of 6 μm) is increasingly displaced by an external force equal to Stokes drag for the cylinder as a function of its angle in a flow travelling along the 'x'-direction. Escape in the flow direction occurs at the maximum transverse trapping efficiency of $\approx Q_x = 0.023$.

agreement with experimental optical forces, and the agreement between experimental and simulated escape of spheres strongly indicates that both the experimental calibration is being performed correctly, and therefore suggesting strongly that the simulations of escape of cylinders are reliable. Since the experimental measurements and simulations of the escape of chromosomes are in reasonable agreement, with the differences attributable to uncertainties in the size and optical properties of the chromosomes, the measurements of escape force for chromosomes are considered reliable. Certainly, they cannot be wrong by the orders of magnitude that agreement with mechanical measurements[1] would require.

The calculated values of Q_{Escape} for isolated chromosomes are smaller than for the microspheres. This may reflect differences in the geometry, morphology, and structural materials of the two, as well as influences of the differences in their refractive indices. The chromosomes are composed of nucleoproteins. Refractometry experiments[54] and modeling of mechanical stress relaxation in chromosomes[55] has indicated that water and other molecules in the surrounding media may penetrate between individual nucleoprotein fibrils whereas the microspheres have a solid structure which prevents the imbibition of water molecules. The behavior of the chromosomes might change in different types of surrounding media, such as the previously observed changes in their refractive indices from 1.4 in a protein containing media to 1.54 in a non-aqueous (Clove oil) media. This change is, perhaps, due to their structural interstices with fine pore sizes that do not permit large molecules to penetrate, and the different amount of water imbibitions in different media[54]. These observations might also explain the changes in Q_{Escape} value for chromosomes in media containing different amounts of methyl cellulose (1 and 3 cP media). We note that the value of the refractive index of the chromosome is highly variable and can be as low as 1.36[37].

Temperature effects of a 1064 nm optical trap. Our results on trapping of isolated chromosomes and microspheres demonstrate

that the Q_{Escape} remains unchanged in the range of the trapping powers used, indicating no significant heating effects on the viscosity of the surrounding medium. Local heating and temperature rise in biological and non-biological specimens confined by optical tweezers at 1064 nm has been studied previously using different techniques[21–25]. Direct temperature measurements based on a microfluorometric technique using temperature-sensitive fluorescent probes showed an average temperature rise of $\approx 1.45°C/100$ mW in trapped micron-size spherical liposome vesicles[21,22]. Temperature rise in trapped Chinese hamster ovary (CHO) cells was measured $\approx 1.15°C/100$ mW with the focal power density of $\approx 10^7$ W/cm². In another study on living cells, the temperature rise was measured to be less than $1.0°C/100$ mW with trapping (*in situ*) powers of up to 400 mW[23].

In our experiments with the 1064 nm continuous wave laser tweezers, with the range of the *in situ* power between $\approx 20–60$ mW, the focal power density would be $\approx 0.9 \times 10^7$ W/cm² at the highest (60 mW) *in situ* power used. Given the previous measurements of the temperature rise in the 1064 nm continuous wave laser trap, and their corresponding range of the *in situ* powers and focal power densities[21–25], the temperature rise in our experiments is in the order of $\approx 1°C/100$ mW in the focal volume. Such a temperature rise would be expected to have little, if any, biological consequence.

In conclusion, the present study defines the potential of optical tweezers as a non-contact sterile method for the measurement of biological forces on spherical and cylindrical objects. The results from our chromosome trapping experiments and the simulation model of trapping cylindrical objects confirm that the amount of force necessary to move a chromosome on the spindle of a dividing cell is likely in the range of 0.1–12 pN.

Methods

Cell culture. Chinese Hamster Ovarian (CHO-K1) cells (ATCC, CCL-61) were grown in advanced minimum essential medium (Gibco) supplemented with 4% fetal bovine serum (FBS). Cells were incubated at 37°C with 5% CO_2.

Chromosome isolation. *Colcemid solution.* We used a 10 mL colcemid solution (Gibco, 15210-040) to prevent spindle formation during mitosis, thus arresting the cells in metaphase. The colcemid solution was prepared in HBSS (Hank's Balanced Salt Solution) and stored at 4°C. A Stock solution was prepared with 5 mM $CaCl_2$ and 1 mM PIPES (Sigma Aldrich, 6757). The pH of the solution was adjusted to 6.5 by adding 1 N NaOH, and the solution was stored at 4°C. A 100 ml working solution was prepared by adding 80 ml of ddH_2O (pH: 6.5) to 10 ml of the stock solution. 11.8 g (≈ 11 ml) of hexylene glycol (Acros Organics, 150340025) was added and mixed well. The final working solution was stored at 4°C.

Isolation procedure. Briefly, the CHO-K1 cells were grown to 80% confluence in three sterile T-150 cell culture flasks (Corning, 430825). Cells were washed with 37°C 1xHBSS(+) solution (Gibco, 14025-092) to remove the floating and rounded cells. Next, the cells were treated with the colcemid solution at 0.06 mcg per mL of growth media, followed by incubation for 2 to 4 hours at 37°C. After incubation, the colcemid containing media with floating cells were transferred to three 50 ml centrifuge tubes and the flasks were washed with cold (4°C) HBSS(-) solution (Gibco, 14175-095) to retrieve additional mitotic cells. This solution was added to three 50 ml centrifuge tubes and placed on ice for 30 minutes to allow dissolution of remaining mitotic spindles.

The tubes were centrifuged at 1000 rpm for 2 minutes at 4°C. The cell pellets were re-suspended in cold (4°C) working solution and transferred to a 15 mL centrifuge tube and centrifuged at 2000 rpm for 3 minutes at 4°C. The cell pellet was re-suspended in ice cold working solution and incubated in a 37°C water bath for approximately 10 minutes allowing the cells to equilibrate with the hypotonic working solution. When the cells swelled so the chromosomes became clearly visible, they were lysed. The cell suspension was transferred to a petri dish and aspirated into a 1 ml syringe with a 25 G needle. The suspension was pushed through the needle to the wall of a 15 ml culture tube. This was repeated several times until most of the cells ruptured yielding a suspension of chromosomes plus some nuclei and unbroken cells. The suspension was filtered through a 10 micron nylon filter to remove nuclei and unbroken cells, placed in 2 mL vials, and stored at 4°C. For experiments that used a more viscous buffer, the chromosome suspension was centrifuged at 3000 rpm for 3 minutes. The supernatant was aspirated and the chromosomes were re-suspended in the desired viscous buffer solution. Vials of chromosomes in viscous buffer were stored at 4°C.

Optical tweezers setup. The optical (laser) tweezers system is similar to one previously described[56]. Briefly, a continuous wave 1064 nm wavelength ytterbium fiber laser (PYL-20M, IPG Photonics) was collimated and steered through a series of mirrors and lenses, and coupled into the epifluorescence port of an inverted microscope (Zeiss Axiovert-135). A dual band laser dichroic mirror (Chroma Technology, z532/1064rpc) was used to reflect the IR laser beam toward the microscope objective while simultaneously transmitting the light from the specimen to a camera. The laser beam was focused through a high numerical aperture (NA=1.4) oil immersion, Phase III, 100X objective (Zeiss Plan-Apochromat). However it has been demonstrated that due to the series of optical aberrations the effective numerical aperture was of the order of 0.8. Several factors contribute to these aberrations. One is that the microscope objective is designed to be used with visible light. Second one is that the depth of the trap influences the results significantly.

Laser exposure and dosimetry. The objective transmission coefficient at 1064 nm wavelength was determined ≈25% based on a three objective measurement method[57]. Prior to, and after each trapping experiment, the power at the back aperture of the objective was measured by removing the objective from the microscope turret and allowing an unobstructed beam to illuminate a 19 mm diameter sensor surface of a Field MaxII TOP power meter coupled to a PowerMax PM3 probe (Coherent Inc., Santa Clara, CA, USA). Laser power in the focal spot was varied from ≈20 to 60 mW in each individual experiment as described in the Results.

Phase contrast imaging and chromosome size measurements. Light from an arc lamp source was collected by the microscope condenser to illuminate the sample. The light from the sample was collected by the objective lens, transmitted through the laser dichroic mirror inside the microscope, and reflected into a digital charged-coupled device (CCD) camera (Hamamatsu, ORCA-R2 C10600-10B) to visualize and capture images of the objects in the field of view. The phase contrast images were acquired with the phase III, 100 X, NA=1.4 objective (Zeiss Plan-Apochromat) and collected by the camera at 30 frame per second (fps). The camera operation and image acquisition processes were controlled with the robotic laser microscopy system software (RoboLase III)[58], and raw images (16-bit) were imported into ImageJ software (1.44p, National Institute of Health, USA) for processing and further analysis. A bandpass filter was placed before the CCD camera in order to cut off IR noise from the trapping laser beam.

The transverse (x and y) image planes were calibrated by measuring known distances in the x and y directions and correlating them with the corresponding number of pixels. For this purpose, a micrometer microscope ruler with 10 μm spacing was used. The calibration yielded ≈16.4 pixels per μm in both x, and y directions. The length and diameter of the individual chromosomes were measured under phase contrast microscopy using a 100X objective. A total number of 77 isolated chromosomes were trapped for measurements in media at 3 cP (centi poise), and 44 chromosomes were trapped at 1 cP. The mean values ± standard deviation (s.d.) of the diameter, length, and aspect ratio (length/radius) of the chromosomes trapped in 1 cp media are 0.939 ± 0.141, 6.44 ± 1.6, and 13.94 ± 3.63, respectively. For the experiments performed in 3 cP media, the respective values of the diameter, length and aspect ratio of the chromosomes are: 0.953 ± 0.173, 6.98 ± 1.88, and 14.9 ± 4.165.

Viscous media preparation. We used methyl cellulose (Sigma Aldrich, M7140, St. Louis, MO, USA) as a chemical reagent to increase the viscosity of the chromosome and microsphere suspension solutions. For this purpose, solutions with different concentrations of methyl cellulose were made by adding various amounts (weight-in-weight ratio) of methyl cellulose to the chromosome suspension solution[59]. Initially, one-third of the solution was heated to 80°C and then the calculated amount of the methyl cellulose powder was added to the heated suspension solution, followed by agitation of the mixture until the particles were evenly dispersed. To reach complete solubilization, the remainder of the solution was added as cold media to lower the temperature of the dispersion. Upon reaching the temperature at which methyl cellulose particles became water soluble, the powder began to hydrate and the viscosity of the solution increased. Next, the solution was cooled to 0–5°C for 20–40 minutes, and continuously agitated for an additional 30 minutes after the proper temperature was reached. A small amount of each final solution (100 μL) was measured for viscosity using an Anton Paar Physica MCR 301 rheometer. The viscosity measurements were performed at room temperature as were all the experiments.

Stage movement and control. A microstepper-motor driven stage for inverted microscopes (Ludl Electronic Products, BioPrecision2, NY, USA) was used to provide controlled transverse motions in x and y directions. The stage was driven by the LabView (LabView 8.5.1, National Instruments, TX, USA) based RoboLase III system software through which the stage could be controlled and driven in x and y directions at given velocities over desired distances with a minimum movement resolution of 200 nm.

Microsphere trapping. Polystyrene microspheres with different diameters were trapped using the 1064 nm optical tweezers system described above. Prior to trapping experiments, the microspheres with known diameters were suspended in glass bottom petri dishes (FluroDish, FD35-100) containing liquid media with known viscosity values. The microspheres subsequently were optically trapped in a range of *in situ* powers. At each power, fluidic viscous drag forces were applied to the trapped

microsphere by driving the microscope stage at known velocities. The velocity of the fluid flow was gradually increased until the trapped microsphere dropped out of the trap at an "escape velocity". This was detected by CCD camera imaging as the microsphere was pulled away from the trapping center by the fluid flow. The polystyrene microspheres with diameters of 4.5 μm (Polysciences Inc., Warrington, PA, USA), 10 μm (Polysciences Inc., Warrington, PA, USA), and 15 μm (Molecular probes, Eugene, OR, USA) were used. The surrounding media viscosity values varied between 1–7 cP for each microsphere size.

In our previous report[59], we have analyzed the effects of adding methyl cellulose on the refractive index of the media. In those experiments, the refractive indices of the viscous solutions were measured using a digital refractometer (Sper Scientific, model 300034, Scottsdale, AZ, USA), with an instrument range of 1.330 to 1.5318 and resolution of 0.0001. No significant changes in the refractive indices of the media containing methyl cellulose were observed upon addition of up to 2% (weight-in-weight ratio). The same methyl cellulose source used in that study was used in the present work (Sigma Aldrich, M7140, St. Louis, MO, USA). In those studies the values of the refractive indices remained unchanged at ≈1.33. Therefore, we used this value for the parameter *n*.

Chromosome trapping. Chromosomes from CHO cells were isolated, suspended in solution, and gently pipetted into glass bottom petri dishes (FluroDish, FD35-100) where they were trapped with the 1064 nm laser. If the chromosomes were twisted, or folded upon themselves, they were not selected for trapping. Once selected for trapping, the chromosome was moved toward the trapping center by movement of the microscope stage. The trap position was indicated by a cross hair in the field of view on the computer screen and the entire chromosome trapping process was monitored by the CCD camera. Often the chromosomes were floating horizontally in the suspension media prior to trapping, and usually they changed to a vertical orientation when the trap was activated. This is likely due to the fact that the trapping point (beam focus) was located near the chromosome tips.

Once a chromosome was in the trap, the microscope stage was driven at a specific velocity in order to apply a known viscous drag force on the chromosome. Similar to trapping of the microspheres, the stage velocity was gradually increased until the trapped chromosome dropped out of the trap. This was evident when the chromosome was swept from the trapping position by the fluid flow as monitored by the CCD camera. Upon increasing the velocity, most of the trapped chromosomes changed their orientation so that they were held horizontally in the fluid flow prior to escaping the trap. The velocity at which the trapped chromosome drops out of the trap is determined to be the "escape velocity".

1. Nicklas, R. B. Measurements of the force produced by the mitotic spindle in anaphase. *J Cell Biol* **97**, 542–548 (1983).
2. Alexander, S. P. & Rieder, C. L. Chromosome motion during attachment to the vertebrate spindle: initial saltatory-like behavior of chromosomes and quantitative analysis of force production by nascent kinetochore fibers. *J Cell Biol* **113**, 805–815 (1991).
3. Marshall, W. F., Marko, J. F., Agard, D. A. & Sedat, J. W. Chromosome elasticity and mitotic polar ejection force measured in living Drosophila embryos by four-dimensional microscopy-based motion analysis. *Curr Biol* **11**, 569–578 (2001).
4. Nicklas, R. B. Chromosome velocity during mitosis as a function of chromosome size and position. *J Cell Biol* **25**, 119–135 (1965).
5. Taylor, E. W. Brownian and saltatory movements of cytoplasmic granules and the movement of anaphase chromosomes. *Proceedings of the Fourth International Congress on Rheology, ed. A. L. Copley, New York: Interscience.* **part 4**, 175–91 (1965).
6. Ferraro-Gideon, J. *et al.* Measurements of forces produced by the mitotic spindle using optical tweezers. *Mol Biol Cell* **24**, 1375–1386 (2013).
7. Grier, D. G. A revolution in optical manipulation. *Nat Photon* **424**, 810–816 (2003).
8. Liang, H. *et al.* Directed Movement of Chromosome Arms and Fragments in Mitotic Newt Lung Cells Using Optical Scissors and Optical Tweezers. *Exp Cell Res* **213**, 308–312 (1994).
9. Kuo, S. C. & Sheetz, M. P. Force of single kinesin molecules measured with optical tweezers. *Science* **260**, 232–4 (1993).
10. Svoboda, K., Schmidt, C. F., Schnapp, B. J. & Block, S. M. Direct observation of kinesin stepping by optical trapping interferometry. *Nature* **365**, 721–7 (1993).
11. König, K. *et al.* Determination of motility forces of human spermatozoa using an 800 nm optical trap. *Cell Mol Biol* **42**, 501–9 (1996).
12. Knöner, G. *et al.* Mechanics of Cellular Adhesion to Artificial Artery Templates. *Biophys J* **91**, 3085–3096 (2006).
13. Ashkin, A., Schutze, K., Dziedzic, J. M., Euteneuer, U. & Schliwa, M. Force generation of organelle transport measured in vivo by an infrared laser trap. *Nature* **348**, 346–348 (1990).
14. Block, S. M., Blair, D. F. & Berg, H. C. Compliance of bacterial flagella measured with optical tweezers. *Nature* **338**, 514–518 (1989).
15. Khatibzadeh, N., Gupta, S., Farrell, B., Brownell, W. E. & Anvari, B. Effects of cholesterol on nano-mechanical properties of the living cell plasma membrane. *Soft Matter* **8**, 8350–8360 (2012).
16. Brownell, W. E., Qian, F. & Anvari, B. Cell Membrane Tethers Generate Mechanical Force in Response to Electrical Stimulation. *Biophys J* **99**, 845–852 (2010).

17. Svoboda, K. & Block, S. M. Biological Applications of Optical Forces. *Annu Rev Biophys Biomol Struct* **23**, 247–285 (1994).
18. Wright, W. H., Sonek, G. J. & Berns, M. W. Parametric study of the forces on microspheres held by optical tweezers. *Appl Opt* **33**, 1735–1748 (1994).
19. Koenig, K., Svaasand, L. O., Tadir, Y., Tromberg, B. J. & Berns, M. W. Optical determination of motility forces in human spermatozoa with laser tweezers. *Proc SPIE* **2926**, 251–256 (1996).
20. Betterton, M. D. & McIntosh, J. R. Regulation of Chromosome Speeds in Mitosis. *Cell Mol Bioeng* **6**, 418–430 (2013).
21. Liu, Y. *et al.* Evidence for localized cell heating induced by infrared optical tweezers. *Biophys J* **68**, 2137–2144 (1995).
22. Liu, Y., Cheng, D. K., Sonek, G. J., Berns, M. W. & Tromberg, B. J. Microfluorometric technique for the determination of localized heating in organic particles. *Appl Phys Lett* **65**, 919–921 (1994).
23. Liu, Y., Sonek, G. J., Berns, M. W. & Tromberg, B. J. Physiological monitoring of optically trapped cells: assessing the effects of confinement by 1064-nm laser tweezers using microfluorometry. *Biophys J* **71**, 2158–2167 (1996).
24. Peterman, E. J. G., Gittes, F. & Schmidt, C. F. Laser-Induced Heating in Optical Traps. *Biophys J* **84**, 1308–1316 (2003).
25. Wurlitzer, S., Lautz, C., Liley, M., Duschl, C. & Fischer, T. M. Micromanipulation of Langmuir-Monolayers with Optical Tweezers. *J Phys Chem B* **105**, 182–187 (2000).
26. Gong, Z., Wang, Z., Li, Y., Lou, L. & Xu, S. Axial deviation of an optically trapped particle in trapping force calibration using the drag force method. *Opt Commun* **273**, 37–42 (2007).
27. Stubblefield, E. & Wray, W. Architecture of the Chinese hamster metaphase chromosome. *Chromosoma* **32**, 262–294 (1971).
28. Ashkin, A. Forces of a single-beam gradient laser trap on a dielectric sphere in the ray optics regime. *Biophys J* **61**, 569–582 (1992).
29. Loke, V. L. Y., Nieminen, T. A., Heckenberg, N. R. & Rubinsztein-Dunlop, H. T-matrix calculation via discrete dipole approximation, point matching and exploiting symmetry. *J Quant Spectrosc Radiat Transf* **110**, 1460–1471 (2009).
30. Nieminen, T. A. *et al.* Optical tweezers computational toolbox. *J Opt A:Pure Appl Opt* **9**, 196–203 (2007).
31. Daban, J.-R. The energy components of stacked chromatin layers explain the morphology, dimensions and mechanical properties of metaphase chromosomes. *J R Soc Interface* **11**, 20131043 (2014).
32. Brennen, C. & Winet, H. Fluid Mechanics of Propulsion by Cilia and Flagella. *Annu Rev Fluid Mech* **9**, 339–398 (1977).
33. Macnab, R. M. Bacterial flagella rotating in bundles: a study in helical geometry. *Proc Natl Acad Sci U.S.A* **74**, 221–225 (1977).
34. Min, K. *et al.* A Novel Gene, ROA, Is Required for Normal Morphogenesis and Discharge of Ascospores in Gibberella zeae. *Eukaryot Cell* **9**, 1495–1503 (2010).
35. Trail, F., Gaffoor, I. & Vogel, S. Ejection mechanics and trajectory of the ascospores of Gibberella zeae (anamorph Fuarium graminearum). *Fungal Genet Biol* **42**, 528–533 (2005).
36. Oster, G. & Perelson, A. Cell protrusions. *In: Frontiers in Mathematical Biology, ed. S. Levin, Berlin:Springer-Verlag* **100**, 53–78 (1994).
37. Sung, Y., Choi, W., Lue, N., Dasari, R. & Yaqoob, Z. Stain-Free Quantification of Chromosomes in Live Cells Using Regularized Tomographic Phase Microscopy. *PLoS ONE* **7**, e49502 (2012).
38. Zickler, D. & Kleckner, N. Meiotic chromosomes: Integrating Structure and Function. *Annu Rev Genet* **33**, 603–754 (1999).
39. Jensen, C. & Bajer, A. Spindle dynamics and arrangement of microtubules. *Chromosoma* **44**, 73–89 (1973).
40. Jensen, C. G. Dynamics of spindle microtubule organization: kinetochore fiber microtubules of plant endosperm. *J Cell Biol* **92**, 540–558 (1982).
41. Svoboda, K. & Block, S. M. Force and velocity measured for single kinesin molecules. *Cell* **77**, 773–784 (1994).
42. Kurachi, M., Hoshi, M. & Tashiro, H. Buckling of a single microtubule by optical trapping forces: direct measurement of microtubule rigidity. *Cell motil cytoskeleton* **30**, 221–228 (1995).
43. Schillers, H., Wälte, M., Urbanova, K. & Oberleithner, H. Real-Time Monitoring of Cell Elasticity Reveals Oscillating Myosin Activity. *Biophys J* **99**, 3639–3646 (2010).
44. Sen, S., Subramanian, S. & Discher, D. E. Indentation and Adhesive Probing of a Cell Membrane with AFM: Theoretical Model and Experiments. *Biophys J* **89**, 3203–3213 (2005).
45. Silberberg, Y. R., Yakubov, G. E., Horton, M. A. & Pelling, A. E. Cell nanomechanics and focal adhesions are regulated by retinol and conjugated linoleic acid in a dose-dependent manner. *Nanotechnology* **20**, 285103 (2009).
46. Fushimi, K. & Verkman, A. S. Low viscosity in the aqueous domain of cell cytoplasm measured by picosecond polarization microfluorimetry. *J Cell Biol* **112**, 719–725 (1991).
47. Luby-Phelps, K. Cytoarchitecture and physical properties of cytoplasm: volume, viscosity, diffusion, intracellular surface area. *Int Rev Cytol* **192**, 189–221 (2000).
48. Kuimova, M. K. *et al.* Imaging intracellular viscosity of a single cell during photoinduced cell death. *Nat Chem* **1**, 69–73 (2009).
49. Mastro, A. M., Babich, M. A., Taylor, W. D. & Keith, A. D. Diffusion of a small molecule in the cytoplasm of mammalian cells. *Proc Natl Acad Sci U.S.A* **81**, 3414–3418 (1984).
50. Periasamy, N., Kao, H. P., Fushimi, K. & Verkman, A. S. Organic osmolytes increase cytoplasmic viscosity in kidney cells. *Am J Physiol Cell Physiol* **263**, 901–907 (1992).
51. Kuimova, M. K., Yahioglu, G., Levitt, J. A. & Suhling, K. Molecular Rotor Measures Viscosity of Live Cells via Fluorescence Lifetime Imaging. *J Am Chem Soc* **130**, 6672–6673 (2008).
52. Nicklas, R. B. The Forces that Move Chromosomes in Mitosis. *Annu Rev Biophys Biophys Chem* **17**, 431–449 (1988).
53. Shimamoto, Y. *et al.* Insights into the Micromechanical Properties of the Metaphase Spindle. *Cell* **145**, 1062–1074 (2011).
54. Barer, R. Refractometry and Interferometry of Living Cells. *J Opt Soc Am* **47**, 545–556 (1957).
55. Poirier, M. G., Nemani, A., Gupta, P., Eroglu, S. & Marko, J. F. Probing Chromosome Structure with Dynamic Force Relaxation. *Phys Rev Lett* **86**, 360–363 (2001).
56. Wu, T. *et al.* A photon-driven micromotor can direct nerve fibre growth. *Nat Photon* **6**, 62–67 (2012).
57. Gomez-Godinez, V. *et al.* Analysis of DNA double-strand break response and chromatin structure in mitosis using laser microirradiation. *Nucleic Acids Res* **38**, e202 (2010).
58. Botvinick, E. L. & Berns, M. W. Internet-based robotic laser scissors and tweezers microscopy. *Microsc Res Tech* **68**, 65–74 (2005).
59. Hyun, N. *et al.* Effects of viscosity on sperm motility studied with optical tweezers. *J Biomed Opt* **17**, 0250051–0250056 (2012).

Author contributions

N.K., H.R.-D. and M.W.B. outlined the research plan. N.K. constructed the experimental setup and optical tweezers system, and performed the microsphere and chromosome laser trapping experiments, collected and analyzed the experimental data. A.B.S., A.A.M.B., V.L., T.A.N. and H.R.-D. performed the numerical calculations, developed the optical trapping model to simulate the microsphere and chromosome trappings with laser tweezers, and provided theoretical supports. N.K. prepared figures 1–2, and A.B.S. prepared figures 3–4. Y.R. and G.M.C. performed cell culture, preparation of the isolated chromosomes and solutions, and performed viscosity measurements with the viscometer. L.Z.S. contributed in microscope stage control/programming. N.K., H.R.-D. and M.W.B. developed the main text of the manuscript in collaboration with A.B.S., A.A.M.B. and T.A.N. All authors reviewed the manuscript.

Additional information

Supplementary information accompanies this paper at http://www.nature.com/scientificreports

Competing financial interests: The authors declare no competing financial interests.

How to cite this article: Khatibzadeh, N. *et al.* Determination of motility forces on isolated chromosomes with laser tweezers. *Sci. Rep.* **4**, 6866; DOI:10.1038/srep06866 (2014).